Adsorption (2015) 21:365–371
DOI 10.1007/s10450-015-9676-6

Enhanced *p*-selectivity from separation of the mixture containing *p*-chloronitrobenzene and *o*-chloronitrobenzene with Sb_2O_3 modified HZSM-5 zeolite

Zhaobing Guo[1,2] · Gang Zeng[1,2] · Jie Liu[1,2] · Fengling Liu[1,2] · Shourong Zheng[3]

Received: 7 February 2015 / Revised: 15 April 2015 / Accepted: 30 May 2015 / Published online: 10 June 2015

Abstract HZSM-5 zeolite was modified with Sb_2O_3 powder, and *p*-selectivity from separation of the mixture containing *p*-chloronitrobenzene (*p*-CNB) and *o*-chloronitrobenzene (*o*-CNB) in modified HZSM-5 zeolite was simultaneously studied. It can be observed that Sb_2O_3 was mainly dispersed on external surface of HZSM-5 zeolite, which might finely narrow pore opening of the zeolite. The maximum adsorption amount of *p*-CNB in the modified zeolite was about 4 molecules per unit cell, which was larger compared to that of *o*-CNB. In addition, the diffusion coefficient of *p*-CNB in Sb_2O_3 modified HZSM-5 at 300 K is observed to be about 531 times higher than that of *o*-CNB. Compared to 85 % *p*-CNB purity recovered from parent HZSM-5 zeolite, the more remarkable differences in adsorption capacity and diffusivity between *p*-CNB and *o*-CNB in Sb_2O_3 modified HZSM-5 led to a higher *p*-CNB purity of 98.4 %, which indicates that *p*-selectivity of HZSM-5 zeolite was significantly enhanced through the modification with Sb_2O_3 powder.

Keywords *p*-Selectivity · Chloronitrobenzene isomers · Sb_2O_3 modified HZSM-5 zeolite

✉ Zhaobing Guo
guozbnuist@163.com

[1] School of Environmental Science and Engineering, Nanjing University of Information Science & Technology, Nanjing 210044, People's Republic of China

[2] Collaborative Innovation Center of Atmospheric Environment and Equipment Technology, Nanjing University of Information Science & Technology, Nanjing 210044, People's Republic of China

[3] State Key Laboratory of Pollution Control and Resource Reuse, School of the Environment, Nanjing University, Nanjing 210093, People's Republic of China

1 Introduction

Chloronitrobenzenes (CNBs) are generally produced by the nitrification of chlorobenzene, which usually includes two isomers *p*-CNB and *o*-CNB. Due to high toxicity and stability, CNBs is expected to be removed before wastewater discharge (Hong et al. 2002). The biological treatment for wastewater containing CNBs is time-consuming. Advanced oxidation processes, such as ozone oxidation (Notario et al. 2013; Pera-Titus et al. 2004), photo-catalysis (Fontaine et al. 2014; Gaya and Abdullah 2008), Fenton oxidation (Yetilmezsoy 2012; Pignatello et al.2006), γ irradiation (Guo et al. 2012) and ultrasonication (Guo et al. 2008), might obtain satisfactory treatment efficiency. While these techniques might produce high cost as well as resource waste. In the viewpoint of clean technology, the recovery of valuable chemicals using adsorbents from the wastewater is superior to degradation techniques. However, the use of polymeric adsorbents or activated carbon as adsorbent is limited due to that the recovered chemicals usually consist of the mixture of *p*-chloronitrobenzene (*p*-CNB) and *o*-chloronitrobenzene (*o*-CNB). Therefore, it is worthy to investigate how to directly obtain a high purity *p*- and *o*-CNB during wastewater treatment. Thus, selective adsorbent is desirable to directly obtain chemicals in high purity from wastewater.

HZSM-5 zeolite is frequently adopted as a selective absorbent in aromatic compounds involved processes due to similar dimensions of the channels to dynamic diameter of benzene molecule (0.58 nm) (Cundy and Cox 2003). HZSM-5 crystals with hierarchical or mesoporous structure have been synthesized and used to improve intracrystalline diffusivities of aromatics (Chu et al. 2009, 2010; Xu et al. 2011; Martinez et al. 2011; Liu et al. 2012; Guo et al. 2015). Our previous study showed that the purity of *p*-CNB

and *o*-CNB using parent HZSM-5 zeolite only reached 85.0 and 95.0 %, respectively (Guo et al. 2005). Therefore, the modification of HZSM-5 zeolite is highly admirable in order to improve *p*-selectivity for CNB isomers.

The modifications of zeolite were mainly carried out by chemical deposition (Zheng et al. 2001) and solid state reaction (Karge and Beyer 1991). Stephan et al. finely controlled pore size of HZSM-5 zeolite by using SiO_2 as deposition agents, which passivated the surface acidity and narrowed the pore size of the zeolite (Reitmeier and Gobin 2009). In addition, two kinds of MoO_3 modified HZSM-5 zeolites were obtained via solid state reaction, which showed similar benzene selectivity in the conversion of methanol to hydrocarbons (Ding et al. 2002). In this contribution, we aim to modify HZSM-5 zeolite with Sb_2O_3 powder, and further study whether to improve selective adsorption for *p*-CNB in Sb_2O_3 modified HZSM-5 zeolite on the basis of the changes in adsorption capacity and diffusivity of *p*- and *o*-CNB compared to those in parent zeolite.

2 Materials and methods

2.1 Materials

p-CNB and *o*-CNB were purchased from Shanghai Chemicals Factory. Sb_2O_3 was obtained from Shanghai No. 4 Reagent & Chemical Co. Ltd. HZSM-5 sample was received from Kailida Power Industry CO. Ltd., with a Si/Al ratio of 48 and average particle diameter of 5 μm.

2.2 Modification of HZSM-5 zeolite

HZSM-5 zeolite and Sb_2O_3 powder were mixed with mass ratio of 4:1 and then grinded uniformly. The mixture was heated to 773 K with a speed of 10 min k^{-1}, and preserved about 2 h before cooling to obtain Sb_2O_3 modified HZSM-5 zeolite.

2.3 Characterization of zeolite

Powder X-ray diffraction (XRD) of modified HZSM-5 was recorded on a Rigaku D/max-RA powder diffraction-meter by using Cu Kα radiation. N_2 adsorption- desorption isotherms for specific surface area and pore distribution of zeolite were conducted on a Micrometrics ASAP 2010 apparatus.

2.4 Adsorption isotherms of CNBs in modified HZSM-5 zeolite

50 mL 100 mg L^{-1} *p*-CNB solution was introduced into the flasks containing Sb_2O_3 modified HZSM-5 zeolite with the mass varying from 10 to 300 mg; or 50 mL 100 mg L^{-1} *o*-CNB solution was transferred into the modified zeolites with different mass from 100 to 1500 mg. After adsorption for 48 h, the zeolite particles were removed by fast filtration and equilibrium concentrations of CNBs in solution were determined spectrophotometrically. The detecting wavelength of *p*-CNB and *o*-CNB was at 285 and 270 nm, respectively.

2.5 Adsorption kinetics of CNBs in modified HZSM-5 zeolite

20 mL distilled water was firstly mixed with 500 mg modified zeolite, 380 mL 53 mg L^{-1} *p*-CNB or 80 mg L^{-1} *o*-CNB solution was then added into the flasks and shaken at the temperature of 278 and 300 K, respectively. Samples were filtered at preset time intervals and residual concentrations of CNBs were measured spectrophotometrically.

2.6 Selective adsorption for *p*-CNB in modified HZSM-5 zeolite

Selective adsorptions for *p*-CNB were conducted in Sb_2O_3 modified HZSM-5 zeolite at 300 and 278 K, respectively. Typically, 20 mL water was mixed with 200 mg Sb_2O_3 modified zeolite at 300 K, 380 mL solution containing 26 mg L^{-1} *p*-CNB and 26 mg L^{-1} *o*-CNB was then introduced in the flask at stirring speed of 200 r min^{-1}. After adsorption, *p*-CNB and *o*-CNB concentrations were measured by HPLC. Chromatographic conditions were as follows: injection volume 5 μL, flow velocity 1 mL min^{-1}, mobile phase consisted of methanol and water with volume ratio of 70:30, detecting temperature 301 K and detection wavelengths 270 nm.

3 Results and discussion

3.1 Characterization of Sb_2O_3 modified HZSM-5 zeolite

The XRD patterns of HZSM-5 zeolite before and after modification are compared in Fig. 1. It is noted that after calcinations of zeolite and Sb_2O_3 powder at 773 K, diffraction peaks assigned to Sb_2O_3 disappeared, while diffraction peaks for HZSM-5 zeolite still remained, suggesting that solid state reaction of Sb_2O_3 with HZSM-5 zeolite presented no influences on HZSM-5 crystalline.

Semi-quantitative analysis of HZSM-5 and Sb_2O_3 mixture before and after calcination was conducted, respectively. It can be found that the content of Sb_2O_3 before calcination was 20 %, while in the modified zeolite that

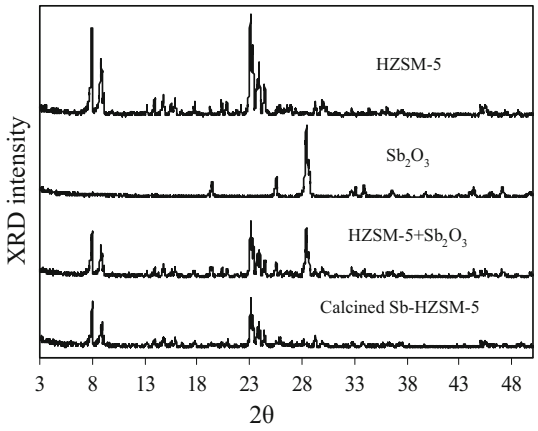

Fig. 1 XRD patterns of HZSM-5 zeolite before and after modification

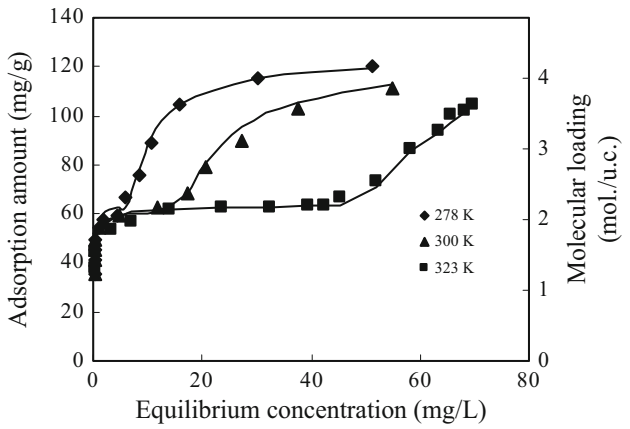

Fig. 2 Adsorption isotherms of *p*-CNB in Sb_2O_3 modified HZSM-5 zeolite at different temperatures

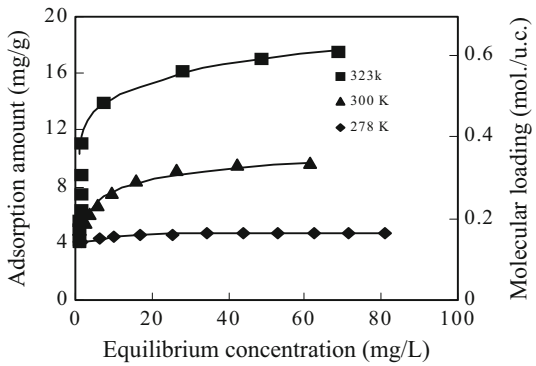

Fig. 3 Adsorption isotherms of *o*-CNB in Sb_2O_3 modified HZSM-5 zeolite at different temperatures

was only 5.04 %. It indicates that the content of Sb_2O_3 decreased markedly during the calcination at 773 K.

Meanwhile, specific surface area and pore distribution of parent and modified HZSM-5 zeolites were determined, respectively. BET surface area and pore volume were 290 $m^2\ g^{-1}$ and 0.101 $cm^3\ g^{-1}$ for parent zeolite (Guo et al. 2005), and 285 $m^2\ g^{-1}$ and 0.097 $cm^3\ g^{-1}$ for Sb_2O_3 modified zeolite. It can be observed that specific surface area and pore volume of HZSM-5 presented a slight change after modification, which suggests that Sb_2O_3 powder was highly dispersed on external surface and pore mouth of HZSM-5 zeolite.

3.2 Adsorption isotherms

The dependencies of adsorption amounts of *p*-CNB and *o*-CNB in Sb_2O_3 modified HZSM-5 zeolites are described at Figs. 2 and 3. In parent and modified zeolites, similar adsorption isotherms for *p*-CNB or *o*-CNB were observed. Based on *p*-CNB adsorption isotherms, two steps occurred at adsorption amounts of about 60 mg g^{-1} (2 mol./u.c.) and 120 mg g^{-1} (4 mol./u.c.), respectively. In contrast, only one step was found in *o*-CNB adsorption isotherms. Step occurrence in adsorption isotherm is usually ascribed to heterogeneous surface of adsorbents or crystalline phase transition caused by the increasing adsorption amount in zeolite (Gregg and Sing 1982). The adsorption isotherms of *p*-CNB and *o*-CNB in Sb_2O_3 modified HZSM-5 zeolites were well fitted the modified bimodal Langmuir adsorption model (Eqs. 1, 2) and Langmuir–Friendlich adsorption model (Eq. 3), respectively (the smooth curves in Figs. 2, 3). The corresponding parameters of *p*- and *o*-CNB are listed in Tables 1 and 2.

$$Q_e = Q_1 b_1 C_e/(1 + b_1 C_e) \quad C_e \le C_s \tag{1}$$

$$Q_e = Q_1 b_1 C_e/(1 + b_1 C_e) + Q_2 b_2 (C_e - C_s)/(1 + b_2 (C_e - C_s)) \quad C_e \ge C_s \tag{2}$$

where Q_e was *p*-CNB adsorption amount (mg g^{-1}) at equilibrium concentration C_e (mg L^{-1}); Cs was equilibrium concentration at which the first step ended (mg L^{-1}); Q_1 and Q_2 were *p*-CNB maximum adsorption amounts in different parts of adsorption isotherms (mg g^{-1}); b_1 and b_2 were adsorption parameters.

$$Q_e = Q_0 b C_e^n/(1 + b C_e^n) \tag{3}$$

where Q_e was *o*-CNB adsorption amount (mg g^{-1}) at equilibrium concentration C_e (mg L^{-1}); Q_0 was maximum adsorption amount (mg g^{-1}); b and n were adsorption parameters.

According to Table 1, maximum adsorption amount of *p*-CNB in Sb_2O_3 modified HZSM-5 zeolite was 125 mg g^{-1} (4.3 mol./u.c.), which was approximately equal to that in parent zeolite. Considering four intersections per unit cell in

Table 1 Regression parameters of *p*-CNB adsorption isotherms in Sb_2O_3 modified HZSM-5 zeolite

	Adsorption temperature (K)		
	278	300	320
Q_1			
Adsorption amount (mg g^{-1})	64.5	61.3	64.1
Molecular loading (mol./u.c.)	2.2	2.1	2.2
Q_2			
Adsorption amount (mg g^{-1})	60.8	64.5	61.2
Molecular loading (mol./u.c.)	2.1	2.2	2.1
$Q_1 + Q_2$			
Adsorption amount (mg g^{-1})	125.3	125.8	125.3
Molecular loading (mol./u.c.)	4.3	4.3	4.3
b_1	6.7	6.5	1.4
b_2	0.22	0.1	0.08
C_s (mg L^{-1})	7.5	16	49.5
r^2	0.9481	0.9524	0.9763

Table 2 Regression parameters of *o*-CNB adsorption isotherms in Sb_2O_3 modified HZSM-5 zeolite

	Adsorption temperature (K)		
	278	300	320
Q_0			
Adsorption amount (mg g^{-1})	5.3	12.2	18.2
Molecular loading (mol./u.c.)	0.18	0.43	0.63
b	3.1	0.6	0.45
n	0.25	0.45	0.2
r^2	0.9715	0.9618	0.9981

modified HZSM-5 zeolite, we concluded that *p*-CNB molecules were mainly located at the intersections of modified zeolite channels (Guo et al. 2005; Randall et al. 1993; Koeningsveld et al. 1989). The results suggested that solid state reaction between Sb_2O_3 and HZSM-5 zeolite could not basically interfere with *p*-CNB movement to adsorption sites in the zeolite despite that pore size of modified zeolite was finely narrowed. On the contrary, it is noted from Table 2 that maximum adsorption amounts of *o*-CNB in modified zeolite were 5.3, 12.2 and 18.2 mg g^{-1} at 278, 300 and 320 K, respectively, which were lower than those of *o*-CNB in the parent zeolite (14.6, 21.6 and 24.8 mg g^{-1}) (Guo et al. 2005). This indicated that Sb_2O_3 modification for HZSM-5 zeolite resulted in a significant restraint on *o*-CNB dispersion to the adsorption sites, which was mainly ascribed to the surface resistances of Sb_2O_3 modification on external surface of HZSM-5 zeolite (Tzoulaki et al. 2008a, b). Thus, the decrease in *o*-CNB adsorption enlarged the difference of maximum adsorption amount between *p*- and *o*-CNB in Sb_2O_3 modified HZSM-5 zeolite.

The dependence of adsorption heat on adsorption amount was further studied to make clear the thermodynamic properties of *p*-CNB in Sb_2O_3 modified HZSM-5 zeolite. Based on adsorption isotherms of *p*-CNB, the equivalent adsorption heat of *p*-CNB in the modified zeolite was obtained by Clausius–Clapeyron equation as follow (Olson and Reichman 1996):

$$\Delta H_{ads} = d\ln(C_e)/d(1/T)_{Q=const} \quad (4)$$

where H_{ads} was adsorption heat, C_e was *p*-CNB equilibrium concentration at constant adsorption amount Q, T was the adsorption temperature.

It is noteworthy from Fig. 4 that adsorption heat of *p*-CNB at adsorption amount less than 2 mol./u.c. was about 12.5 kJ mol^{-1}, which was lower than that in parent zeolite (15 kJ mol^{-1}). It might be ascribed to the enhanced hydrophobicity of zeolite surface and the weakened electrostatic force inside the pores of Sb_2O_3 modified zeolite. In addition, solid state reaction between Sb_2O_3 powder and zeolite slightly narrowed the pore size of zeolite and enhanced the resistance on the inner wall of pore channels, which also led to a decrease in adsorption heat. At *p*-CNB adsorption amount about 2 mol./u.c., adsorption heat in modified zeolite increased to 30 kJ mol^{-1}, however, it was still lower than that in the parent zeolites (32 kJ mol^{-1}). The sharp increase of adsorption heat was attributed to enhanced repulsive force between the adsorbed *p*-CNB molecules. At adsorption amount about 4 mol./u.c., some *p*-CNB molecules were adsorbed in zeolite channels, and the increased repulsive force between the adsorbed molecules and the zeolite framework played as the driving force. The whole adsorption system needed more energy to overcome the energy barrier in the pore channels. Additionally, at adsorption loading above 4 mol./u.c., *p*-CNB is

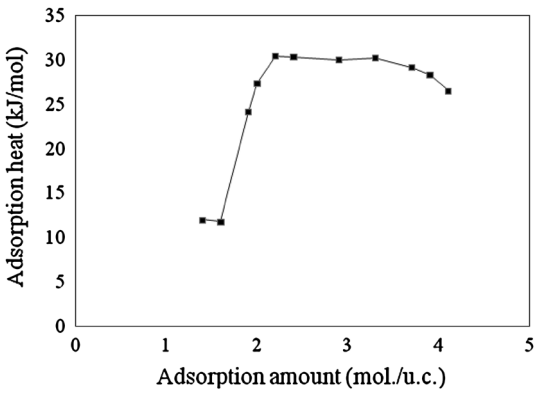

Fig. 4 Dependence of adsorption heats on *p*-CNB loading in Sb_2O_3 modified zeolites

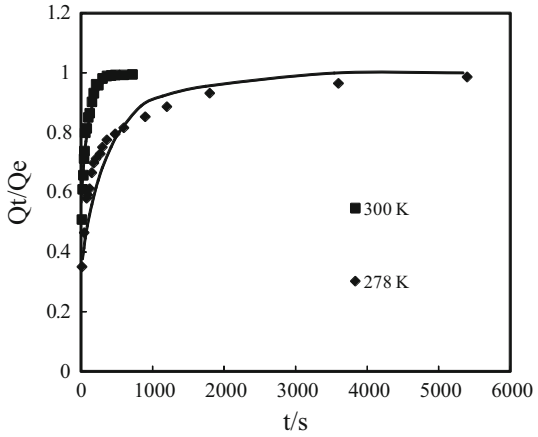

Fig. 5 Diffusion of *p*-CNB in Sb_2O_3 modified HZSM-5 zeolite at different temperatures

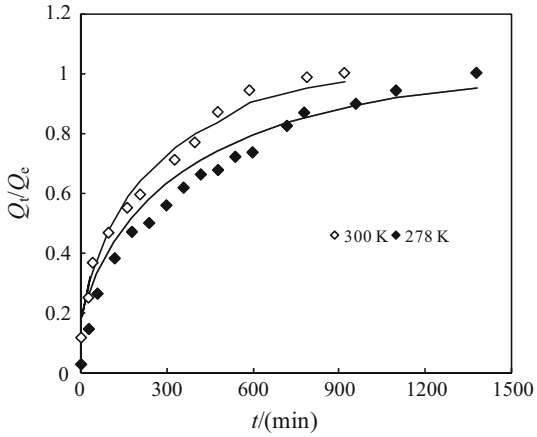

Fig. 6 Diffusion of *o*-CNB in Sb_2O_3 modified HZSM-5 zeolite at different temperatures

expected to be adsorbed on external surface of zeolite, which resulted in a significant decrease in adsorption heat.

3.3 Adsorption kinetics

The diffusion curves of *p*- and *o*-CNB in Sb_2O_3 modified HZSM-5 zeolites at different temperatures are shown in Figs. 5 and 6, respectively. The diffusion of *p*-CNB in MFI type zeolite was usually controlled by internal diffusion process (Farrell et al. 2003). Consequently, the diffusion process of CNB molecules in Sb_2O_3 modified HZSM-5 zeolite might be described by using homogeneous solid diffusion model (Eq. 5)(Cavalcante and Ruthven 1995).

$$\frac{Q_t}{Q_\infty} = 1 - \frac{6}{\pi^2}\sum_{n=1}^{\infty}\frac{1}{n^2}\exp\left(-\frac{n^2\pi^2 Dt}{r^2}\right) \quad (5)$$

where Q_t (mg g^{-1}) denoted *p*-CNB adsorption amount at time *t* (s), Q_∞ (mg g^{-1}) was maximum adsorption amount, *r* was zeolite radius and *D* was diffusion coefficient.

The diffusion coefficients of *p*-CNB in the modified zeolite were 1.2×10^{-15} and 8.5×10^{-15} m^2 s^{-1} at 278 and 300 K, with equilibrium adsorption amounts of *p*-CNB at 51.2 and 49.5 mg g^{-1}, respectively. It is indicated that diffusion coefficient of *p*-CNB in modified zeolite increased by seven times with the temperature increasing from 278 K to 300 K, which was almost identical to that in parent zeolite (6.5). This suggested that surface resistance and slight narrowing in pore size of modified zeolite were insufficient to substantially change diffusion activation energy of *p*-CNB (E_{after} = 61.3 kJ mol^{-1}, E_{before} = 58.6 kJ mol^{-1}, calculated by the Arrhenius equation), which indicates that *p*-CNB diffusion inside the zeolite pores controlled the uptake process.

In addition, the diffusion coefficients of *o*-CNB in the modified zeolite were found to be 4×10^{-18} and 1.6×10^{-17} m^2 s^{-1} at 278 and 300 K, with *o*-CNB equilibrium adsorption amounts at 10.8 and 11 mg g^{-1}, respectively. The enhanced diffusion coefficient with increasing temperature resulted in an increase in diffusion activation energy of *o*-CNB in the modified zeolite (E_{after} = 83.0 kJ mol^{-1}; E_{before} = 63.5 kJ mol^{-1}). This implied that more *o*-CNB diffusion restriction had been achieved in Sb_2O_3 modified zeolite compared to that in parent zeolite.

It is noteworthy that the diffusion of *p*- and *o*-CNB in HZSM-5 zeolite is of configurational diffusion due to that kinetic diameter of benzene ring (0.58 nm) is close to the pore size of HZSM-5 zeolite. The small difference in molecular diameter of *p*-CNB (0.58 nm) and *o*-CNB (0.79 nm), surface barriers as well as the slight change in pore size of modified zeolite might result in a significant effect on the diffusivity of CNB molecules (Kärger et al. 2014; Kärger and Ruthven 1992). In this study, the surface barriers and finely narrowed pore size of HZSM-5 zeolite caused by Sb_2O_3 modification as well as the difference of kinetic diameter between *p*- and *o*-CNB molecules led to a diffusion coefficient of *p*-CNB 433 times larger compared to that of *o*-CNB. Therefore, it can be concluded that surface barrier as well as the correlation between the diameter of molecules and pore size of zeolite were the main factors in controlling CNB diffusion.

3.4 Selective adsorption for *p*-CNB

The differences in adsorption amount and diffusion coefficient between *p*-CNB and *o*-CNB in the zeolite were significantly improved by the modification with Sb_2O_3, which was favorable to selective adsorption for *p*-CNB. The adsorption and diffusion behaviors of bicomponent CNBs in Sb_2O_3 modified HZSM-5 zeolite are presented in Fig. 7.

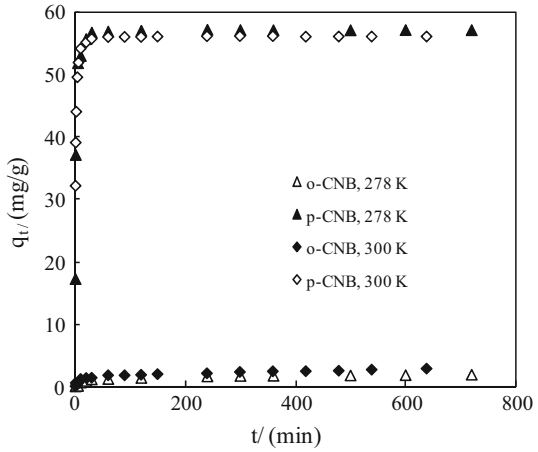

Fig. 7 Time resolved uptakes of *p*- and *o*-CNB in Sb_2O_3 modified HZSM-5 zeolite at different temperatures

It is noted that *p*-CNB adsorption from CNB mixture in Sb_2O_3 modified HZSM-5 at 278 and 300 K reached equilibrium within 15–20 min, the equilibrium concentration of which were 1.4 and 1.3 mg L^{-1} with the corresponding adsorption amounts at 57.1 and 56.3 mg g^{-1}, respectively. According to the fitting results of *single*-component *p*-CNB adsorption isotherms, we found that *p*-CNB adsorption capacities were 56.5 and 56.7 mg g^{-1} at the concentrations of 1.4 mg L^{-1} at 278 K and 1.3 mg L^{-1} at 300 K, respectively. This indicated that the presence of *o*-CNB basically had no effect on *p*-CNB adsorption process. However, the adsorption equilibration time of *o*-CNB in mixture in Sb_2O_3 modified HZSM-5 was much longer than 10 h. The equilibrium concentrations of *o*-CNB at 278 and 300 K were 30.5 and 24.2 mg L^{-1}, and the corresponding adsorption amounts were 1.9 and 2.8 mg g^{-1}, respectively. Compared to adsorption amounts of *single*-component *o*-CNB (4.7 and 9.0 mg g^{-1}) at 278 and 300 K, adsorption amounts of *o*-CNB in CNB mixture decreased by 60 and 69 %, respectively. It can be concluded that the *o*-CNB was at a complete disadvantage in adsorption against *p*-CNB for its antagonistic effect on *p*-CNB.

The simulation of diffusion curves for *p*- or *o*-CNB in mixture in Sb_2O_3 modified zeolite showed that diffusion coefficients of *p*-CNB at 278 and 300 K were 1.0×10^{-15} and 4.0×10^{-15} m^2 s^{-1}, respectively, corresponding to *single*-component *p*-CNB of 1.2×10^{-15} and 5.2×10^{-15} m^2 s^{-1} at similar adsorption amounts. Meanwhile, the diffusion coefficients of *o*-CNB in mixture at 278 and 300 K were 1.4×10^{-18} and 6.3×10^{-18} m^2 s^{-1}, respectively, while the diffusion coefficient of *single*-component *o*-CNB was 1.3×10^{-17} m^2 s^{-1} at 300 K. The results illustrated that the diffusivities of *p*-CNB in CNBs mixture in Sb_2O_3 modified zeolite slightly decreased, but the diffusion process of *o*-CNB was restrained. Therefore, the presence of *p*-CNB inhibited *o*-CNB diffusion. Also, *o*-CNB is expected to slow down the movement of *p*-CNB in the modified zeolite (Krishna et al. 2004; Krishna et al. 2008; Titze et al. 2014).

During competitive adsorption of *p*- and *o*-CNB, a high *p*-selectivity in Sb_2O_3 modified zeolite was achieved. This is ascribed to that the relatively small dynamic diameter of *p*-CNB led to a faster diffusion rate and a prior access to channel intersections. However, *o*-CNB had no competitive advantage into zeolite channels due to the pore mouth blocking of Sb_2O_3 modified zeolite and the surface barrier caused by Sb_2O_3 modification. The enlarged differences in adsorption and diffusivity between *p*-CNB and *o*-CNB in Sb_2O_3 modified zeolite were favorable for CNB isomers separation and thereby enhancing selective adsorption for *p*-CNB.

At 300 K, the equilibrium concentrations of *p*- and *o*-CNB in mixture were 1.3 and 24.2 mg L^{-1} and the corresponding adsorption amounts in Sb_2O_3 modified zeolite were 56.3 and 2.8 mg g^{-1}. Consequently, 94.9 % *p*-CNB and 95.3 % *o*-CNB could be recovered after subsequent treatment. Especially, after about 20 min adsorption when *p*-CNB just reached equilibrium, *p*-CNB with the purity of 97.7 % was acquired. Similarly, at 278 K, the equilibrium concentrations of *p*- and *o*- CNB in mixture were 1.4 and 30.5 mg L^{-1}, and the corresponding adsorption capacities were 57.1 and 1.9 mg g^{-1}, respectively. As a result, 94.4 % *p*-CNB and 95.6 % *o*-CNB could be obtained. Under the optimal condition, the purity of *p*-CNB could increase up to 98.4 %. The results indicated that Sb_2O_3 modified HZSM-5 zeolite could obtain higher selectivity for *p*-CNB compared to that in the parent zeolite.

4 Conclusions

The modification of HZSM-5 zeolite using Sb_2O_3 powder was proved to be an effective method to enhance selective adsorption for *p*-CNB. Sb_2O_3 was highly dispersed on external surface of HZSM-5 zeolite. Additionally, Sb_2O_3 covered a portion of externally accessible acid sites, and led to a slight narrow of pore opening of the zeolite without significantly affecting its adsorption capacity and diffusivity for *p*-CNB. However, *o*-CNB molecules were markedly restrained during adsorption process. Therefore, the differences in adsorption and diffusion between *p*- and *o*-CNB in Sb_2O_3 modified zeolites were enlarged. As a result, the higher selectivity for *p*-CNB was achieved in Sb_2O_3 modified zeolite compared to that in the parent zeolite.

Acknowledgments We gratefully acknowledge supports from National Natural Science Foundation of China (41373023); Jiangsu

Province research prospective joint research project (BY2013007-03); Jiangsu Province Environmental Protection Research Project (2014t016); Jiangsu Province "333 high-level talents project" and "Six major talent Summit"; A project funded by the Priority Academic Program Development of Jiangsu Higher Education Institutions.

References

Cavalcante, C.L., Ruthven, D.M.: Adsorption of branched and cyclic paraffins in silicalite. 2. Kinetics. Ind. Eng. Chem. Res. **34**, 185–191 (1995)

Chu, N.B., Yang, J.H., Li, C.Y., Cui, J.Y., Zhao, Q.Y., Yin, X.Y., Lu, J.M., Wang, J.Q.: An unusual hierarchical ZSM-5 microsphere with good catalytic performance in methane dehydroaromatization. Microporous Mesoporous Mater. **118**, 169–175 (2009)

Chu, N.B., Yang, J.H., Wang, J.Q., Yu, S.X., Lu, J.M., Zhang, Y., Yin, D.H.: A feasible way to enhance effectively the catalytic performance of methane dehydroaromatization. Catal. Commun. **11**, 513–517 (2010)

Cundy, C.S., Cox, P.A.: The dydrothermal synthesis of zeolites: history and development from the earliest days to the present time. Chem. Rev. **103**, 663–702 (2003)

Ding, W., Meitzner, G.D., Iglesia, E.: The effects of silanation of external acid sites on the structure and catalytic behavior of Mo/H-ZSM-5. J. Catal. **206**, 14–22 (2002)

Farrell, J., Manspeaker, C., Luo, J.: Understanding competitive adsorption of water and trichloroethylene in a high-silica Y zeolite. Microporous Mesoporous Mater. **59**, 205–214 (2003)

Fontaine, B., Drosos, M., Mazzei, P.: Copolymerization of 2,4-dichlorophenol with humic substances by oxidative and photo-oxidative biomimetic catalysis. Environ. Sci. Pollut. Res. **21**, 1–9 (2014)

Gaya, U.I., Abdullah, A.H.: Heterogeneous photocatalytic degradation of organic contaminants over titanium dioxide: a review of fundamentals, progress and problems. J. Photochem. Photobiol. C **9**, 1–12 (2008)

Gregg, S.J., Sing, K.S.W.: Adsorption, Surface Area and Porosity, pp. 84–94. Academic Press, London (1982)

Guo, Z.B., Chen, S.L., Liu, F.L., Wang, J.J., Shen, X.Y., Zheng, S.R.: Recovery of *p*-nitrotoluene by selective adsorption using MFI type zeolites. Adsorption **21**(1–2), 143–151 (2015)

Guo, Z.B., Dong, Q.Y., He, D.L., Zhang, C.Z.: Gamma radiation for treatment of bisphenol A solution in presence of different additives. Chem. Eng. J. **183**, 10–14 (2012)

Guo, Z.B., Feng, R., Li, J.H., Zheng, Z., Zheng, Y.F.: Degradation of 2,4-dinitrophenol by combining sonolysis and different additives. J. Hazard. Mater. **158**, 164–169 (2008)

Guo, Z.B., Zheng, S.R., Zheng, Z., Jiang, F., Hu, W.Y., Ni, L.X.: Selective adsorption of p-chloronitrobenzene from aqueous mixture of p-chloronitrobenzene and o-chloronitrobenzene using HZSM-5 zeolite. Water Res. **39**, 1174–1182 (2005)

Hong, S.K., Anestis, D.K., Ball, J.G.: In vitro nephrotoxicity induced by chloronitro-benzenes in renal cortical slices from Fischer 344 rats. Toxicol. Lett. **129**, 133–141 (2002)

Karge, H.G., Beyer, H.K.: Zeolite chemistry and catalysis. In: Jacobs, P.A., Jaeger, N.I., Kubelková, L., Wichterlová, B. (eds.) Studies in Surface Science and Catalysis, vol. 69, p. 43. Elsevier, Amsterdam (1991)

Kärger, J., Binder, T., Chmelik, C., Hibbe, F., Krautscheid, H., Krishna, R., Weitkamp, J.: Microimaging of transient guest profiles to monitor mass transfer in nanoporous materials. Nature Mater. **13**, 333–343 (2014)

Kärger, J., Ruthven, D.M.: Diffusion in Zeolites and Other Microporous Solids. Wiley, New York (1992)

Krishna, R., Paschek, D., Baur, R.: Modeling the occupancy dependence of diffusivities in zeolites. Microporous Mesoporous Mater. **76**, 233–246 (2004)

Krishna, R., Li, S.G., van Baten, J.M., Falconer, J.L., Noble, R.D.: Investigation of slowing-down and speeding-up effects in binary mixture permeation across SAPO-34 and MFI membranes. Sep. Purif. Technol. **60**, 230–236 (2008)

Liu, H., Yang, S., Hu, J., Shang, F.P., Li, Z.F., Xu, C., Guan, J.Q., Kan, Q.B.: A comparison study of mesoporous Mo/H-ZSM-5 and conventional Mo/H-ZSM-5 catalysts in methane non-oxidative aromatization. Fuel Process. Technol. **96**, 195–202 (2012)

Martinez, A., Peris, E., Derewinski, M., Burkat-Dulak, A.: Improvement of catalyst stability during methane dehydroaromatization on Mo/HZSM-5 comprising intracrystalline mesopores. Catal. Today **169**, 75–84 (2011)

Notario, A., Bravo, I., Adame, J.A.: Behaviour and variability of local and regiooxidant levels measured in a polluted area in central-southern of Iberian Peninsula. Environ. Sci. Pollut. Res. **20**(1), 188–200 (2013)

Olson, D.H., Reichman, P.T.: Structure-related paraffin sorption in ZSM-5. Zeolites **17**, 434–436 (1996)

Pera-Titus, M., Verónica, M., Miguel, A.B.: Degradation of chlorophenols by means of advanced oxidation processes: a general review. Appl. Catal. B **47**, 219–256 (2004)

Pignatello, J.J., Esther, O., Allison, M.: Advanced oxidation processes for organic contaminant destruction based on the fenton reaction and related chemistry. Crit. Rev. Environ. Sci. Technol. **36**, 61–84 (2006)

Randall, Q.S., Alexis, T.B., Doros, N.: Prediction of adsorption of aromatic hydrocarbons in silicalite from grand canonical Monte Carlo simulations with biased insertions. J. Phys. Chem. **97**(51), 13742–13752 (1993)

Reitmeier, S.J., Gobin, O.C.: Enhancement of sorption processes in the zeolite H-ZSM-5 by postsynthetic surface modification. Angew. Chem. Int. Ed. **48**, 533–538 (2009)

Titze, T., Chmelik, C., Kärger, J., van Baten, J.M., Krishna, R.: Uncommon synergy between adsorption and diffusion of hexane isomer mixtures in MFI zeolite induced by configurational entropy effects. J. Phys. Chem. C **118**, 2660–2665 (2014)

Tzoulaki, D., Heinke, L., Schmidt, W., Wilczok, U., Kärger, J.: Exploring crystal morphology of nanoporous hosts from time-dependent guest profiles. Angew. Chem. Int. Ed. **47**, 3954–3957 (2008a)

Tzoulaki, D., Schmidt, W., Wilezok, U., Karger, J.: Formation of surface barriers on silicalite-1 crystal fragments by residual water vapour as probed with isobutane by interference microscopy. Microporous Mesoporous Mater. **110**, 72–76 (2008b)

van Koeningsveld, H., Tuinstra, F., van Bekkum, H., Jansen, J.C.: The location of p-xylene in a sinlge crystal of zeolite H-ZSM-5 with a new, sorbate-induced, orthorhombic framework symmetry. Acta Crystallogr. Sect. B **45**, 423–431 (1989)

Xu, C., Liu, H., Jia, M.J., Guan, J.Q., Wu, S.J., Wu, T.H., Kan, Q.B.: Methane non-oxidative aromatization on Mo/ZSM-5: effect of adding triethoxyphenylsilanes into the synthesis system of ZSM-5. Appl. Surf. Sci. **257**, 2448–2454 (2011)

Yetilmezsoy, K.: Fuzzy-logic modeling of Fenton's oxidation of anaerobically pretreated poultry manure wastewater. Environ. Sci. Pollut. Res. **19**(6), 2227–2237 (2012)

Zheng, S., Heydenrych, H., Röger, P., Jentys, A., Lercher, J.A.: Structural properties and sieving effects of surface modified ZSM-5. Stud. Surf. Sci. Catal. **135**, 214–223 (2001)